Fizika Nizkikh Temperatur, 2007, v. 33, Nos. 6/7, p. 783–789

Orientational order parameter in CO_2-based alloys with rare gases from THEED data: pure CO_2

V.V. Danchuk, A.A. Solodovnik, and M.A. Strzhemechny

B. Verkin Institute for Low Temperature Physics and Engineering of the National Academy of Sciences of Ukraine
47 Lenin Ave., Kharkov 61103, Ukraine
E-mail: strzhemechny@ilt.kharkov.ua

Received February 7, 2007

Using the transmission high-energy electron diffraction technique, we studied the temperature dependence of the diffraction reflection intensities from the solid phase of CO_2. To deduce absolute values of the orientational order parameter, we modified the existing reconstruction method to account for the triatomic shape of the molecule. It is shown that for triatomics solids a higher-rank order parameter, η_4, is important and cannot be neglected. Application of the modified approach yielded η and η_4 values as a function of temperature over the range from 6 to 70 K. Both orientational order parameters proved to be a nonmonotone function of temperature.

PACS: **61.14.–x** Electron diffraction and scattering;
61.14.Dc Theories of diffraction and scattering;
75.40.Gb Dynamic properties (dynamic susceptibility, spin waves, spin diffusion, dynamic scaling, etc.).

Keywords: electron diffraction, rare gases alloys, orientational order.

1. Introduction

The problem of the orientational order in mixed cryocrystals consisting of two components, one of which is a linear molecule and the other is a rare gas atom, still remains an important issue for random systems. Usually, orientational order is quantitatively described by the orientational order parameter (OOP), which in a solid made up of linear molecules is defined as

$$\eta = \langle P_2(\cos\theta)\rangle, \qquad (1)$$

where $P_2(x)$ is the Legendre polynomial and θ is the angle the molecule in a specific sublattice of an orientationally ordered structure makes with the axis of the preferable orientation of this molecule. The resonance methods, which are traditionally used to determine η, fail for mixed systems and, actually, the only constructive option is to utilize diffraction data for that purpose. In our earlier paper devoted to this problem [1] we outlined the general approach for a specific case of Ar–CO_2 mixed crystals. This approach has been developed to a quite high precision for diatomics and then successfully applied for the reconstruction of η in α-N_2 from our own powder x-ray diffraction measurements [2] and in the orientationally ordered almost pure para-deuterium [3] from the old neutron diffraction data of Yarnell et al. [4]. As we will show below, application of this approach even to symmetric triatomics requires further development; electron diffraction data were used to tentatively reconstruct η in the noncubic diatomic crystal of α-oxygen [5]. Since some new problems, which are inherent even in pure triatomic CO_2, need detailed consideration, in this paper we start with the orientational order in pure CO_2 crystal. We expected that our approach might yield qualitatively new results compared to those that can be obtained on diatomic crystals. At the same time, considering the fact that transmissive high-energy electron diffraction data were not so far obtained with the aim of obtaining reliable integrated intensities, we made new accurate transmission high-energy electron diffraction measurements on solid CO_2 over the temperature range from 5 to 70 K, close to the sublimation threshold.

2. Theory

In the theory developed below we will make use of the fact that the structure of CO_2 over the entire domain of its sold state is $Pa\bar{3}$.

The integrated intensity of scattered electrons can be represented in the form [6,7].

$$I \propto \Phi(\theta) P(\mathbf{q}) f_T(\mathbf{q}) \left| \sum_s F_s(\mathbf{q}) \mathrm{e}^{2\pi i \mathbf{q}\mathbf{R}_s} \right|^2 , \qquad (2)$$

where summation runs over positions $\mathbf{R}_s$ occupied by all C and O atoms in the elementary cell; $\mathbf{q}$ is the momentum transfer vector; θ is the diffraction angle; $\Phi(\theta)$ accounts for the geometric factor of data taking; $P(\mathbf{q})$ is the repetition factor for a particular reflection; $f_T(\mathbf{q})$ is the Debye–Waller temperature factor; and F_s is the structure amplitude.

Let us first consider the scattering amplitude F_s. Taking into account the fact that the carbons occupy the sites of a fcc array and summing over pairs of oxygen atoms in each molecule (sublattice) we obtain for the structure amplitude

$$F(\mathbf{q}) = \sum_c \mathrm{e}^{2\pi i \mathbf{q}\mathbf{R}_c} [f_C(\mathbf{q}) + 2 f_O(\mathbf{q}) \cos \xi(\mathbf{q}\mathbf{w}_c)] \ . \qquad (3)$$

Here $f_C(\mathbf{q})$ and $f_O(\mathbf{q})$ are the atomic scattering factors for the carbon and oxygen atoms, respectively; summation runs over the four sublattices c of the $Pa\bar{3}$ structure with $\mathbf{R}_c$ being the centers of the four molecules in the four sublattices; $\mathbf{w}_c$ is the momentary direction of the unit vector along the respective molecular axis in sublattice c;

$$\xi = 2\pi d / a(T) \ , \qquad (4)$$

where $d = 1.1599$ Å is the C = 0 bond length in the CO_2 molecule [8] and $a(T)$ is the lattice parameter, which is temperature dependent. At temperatures close to zero, the powder x-ray lattice parameter [9] is $a = 5.5542$ Å and $\xi = 1.31214$. Since the summing in Eq. (3) goes over all elementarily cells, the integrated intensity in Eq. (2) will contain a self-averaged value of the cosine. This averaged cosine can be expanded [1] in spherical harmonics [10], which will yield for the scattering amplitude

$$F(\mathbf{q}) = \sum_c e^{2\pi i \mathbf{q}\mathbf{R}_c} [f_C(\mathbf{q}) +$$

$$+ 2 f_O(\mathbf{q}) \sum_{\text{even } l \geq 0} i^{\,l} (2l+1) j_l(\xi q) (\mathbf{C}_l(\mathbf{n}) \cdot \langle \mathbf{C}_l(\mathbf{w}_c) \rangle)] . \qquad (5)$$

Here the brackets denote thermodynamic averaging; $j_l(y)$ are the spherical Bessel functions; summing in the inner sum is over even l; $C_{lm}(\mathbf{n})$ and $\mathbf{C}_l(\mathbf{n})$ are Racah's spherical harmonics and the respective spherical tensors [8]; $\mathbf{n}$ and q are unit vector and the length of the momentum transfer: $\mathbf{q} \equiv q\mathbf{n}$; and

$$(\mathbf{C}_l(\mathbf{n}) \cdot \mathbf{C}_l(\mathbf{w}_c)) = \sum_{m=-l} C^*_{lm}(\mathbf{n}) C_{lm}(\mathbf{w}_c) , \qquad (6)$$

is the scalar product of two spherical tensors of rank l.

The geometric factor $\Phi(\theta)$ in Eq. (2) is determined by the geometry and intensity registration method. In our case [12], this factor is proportional to the specific inter-plane separation squared:

$$\Phi(\theta) \propto d^2_{hkl} = a^2 / H^2 = \frac{\lambda^2}{4 \sin^{\,2}\theta} , \qquad (7)$$

where $H^2 = h^2 + k^2 + l^2$ and λ is the electron wavelength.

The temperature factor $f_T(\mathbf{q})$ in Eq. (2) is chosen in the standard Debye approximation [12], ideally applicable for our case with the Debye temperature Θ equal [13] to (151.8 ± 1.5) K.

The main reason why the approach under discussion was efficient and simple to apply for all diatomic crystals such as nitrogen [2], deuterium [3], or oxygen [5,11] is the small value of the parameter ξ as defined in Eq. (4), which permitted us to leave only the first two terms in the expansion in Eq. (5) to stay within an accuracy better than 2–3%. In a triatomic crystal such as CO_2 the parameter ξ is roughly twice as large, which does not allow so short a truncation. Therefore, we have to consider higher terms, the thermodynamic interpretation of which is not so simple as that of the rank-2 term, which yields the standard orientational order parameter η.

Let us start our analysis of Eq. (5) with the first two terms of the series in l. It can be shown [2] (see Appendix A) that the $l = 2$ term after averagingr yields precisely the orientational order parameter as defined in Eq. (1):

$$\langle C_{2m}(\mathbf{w}_c) \rangle = \eta C_{2m}(\mathbf{m}_c) , \qquad (8)$$

where $\mathbf{m}_c$ is the unit vectors along the preferable orientation of the molecule in sublattice c, i.e., along the corresponding cube diagonal in the $Pa\bar{3}$ structure. Moreover [10],

$$(\mathbf{C}_2(\mathbf{n}) \cdot \mathbf{C}_2(\mathbf{m}_c)) = P_2(\mathbf{n} \cdot \mathbf{m}_c) , \qquad (9)$$

where P_2 is again the Legendre polynomial. Finally, the first two terms yield [2]:

$$F_s^{(0)} + F_s^{(2)} =$$

$$= \begin{cases} 4 f_C(\mathbf{q}) + 8 f_O(\mathbf{q}) j_0(\alpha q) & \text{regular reflections,} \\ -10 f_O(\mathbf{q}) \eta j_2(\alpha q) Q_2(\mathbf{q}) & \text{superstructure reflections,} \end{cases} \qquad (10)$$

where we define

$$Q_N(\mathbf{q}) = \sum_c \mathrm{e}^{2\pi i \mathbf{q}\mathbf{R}_c} P_N(\mathbf{n} \cdot \mathbf{m}_c) . \qquad (11)$$

The term with $l = 4$ in Eq. (5) differ from the previous that with $l = 2$ in that not only the $m = 0$ component in the intrinsic reference frame will survive (see Appendix A). making use of Eq. (A.1) we can write the third ($l = 4$) term of the scattering amplitude in the form

$$F_s^{(4)} = 18 f_O(\mathbf{q}) j_4(\alpha q) \{\eta_4 Q_4(\mathbf{q}) +$$

$$+ \zeta_{43} \sum_c e^{2\pi i \mathbf{q}\mathbf{R}_c} [C_{43}(\mathbf{n}_0) - C_{43\bar{3}}(\mathbf{n}_0)]\} \qquad (12)$$

with the anisotropy parameter ζ_{43} defined in Eq. (A.5).

The corresponding expression for the $l = 6$ contribution to the scattering amplitude can be obtained in a similar way with that difference that the final formula analogous to Eq. (12) will contain also terms with $m = \pm 6$:

$$F_s^{(6)} = -26 f_O(\mathbf{q}) j_6(\alpha q)\{\eta_6 Q_6(\mathbf{q}) +$$
$$+ \zeta_{63} \sum_c e^{2\pi i \mathbf{q}\mathbf{R}_c} [C_{63}(\mathbf{n}_0) - C_{63\bar{3}}(\mathbf{n}_0)] +$$
$$+ \zeta_{66} \sum_c e^{2\pi \mathbf{q}\mathbf{R}_c} [C_{66}(\mathbf{n}_0) + C_{66\bar{6}}(\mathbf{n}_0)]\}, \qquad (13)$$

where η_6 is the rank-6 order parameter, defined similarly as η_4, and the two possible rank-6 anisotropy parameters are

$$\zeta_{63} \equiv \frac{1}{2}[\langle C_{63}(\mathbf{w}_{c0})\rangle - \langle C_{63\bar{3}}(\mathbf{w}_{c0})\rangle], \qquad (14)$$

$$\zeta_{66} \equiv \frac{1}{2}[\langle C_{66}(\mathbf{w}_{c0})\rangle + \langle C_{66\bar{6}}(\mathbf{w}_{c0})\rangle]. \qquad (15)$$

The presence of the anisotropy parameters in addition to a few orientational order parameters seems to considerably complicate the task of reconstructing all these quantities from diffraction intensities. However, we will further show that the anisotropy parameters in the triatomic cryocrystal CO_2 are negligible compared to the respective order parameters and can be thus discarded (see also Appendix B). This assertion will be verified when making the relevant calculations.

3. Experimental

The structure of thin CO_2 films was studied by transmission high-energy electron diffraction (THEED) with the aid of an EG-100A Electronograph equipped with a special liquid helium cryostat. The film samples were prepared *in situ* inside the column of the instrument by depositing the CO_2 gas at room temperature onto a composite substrate (cooled down to 45 K), which consisted of two parallel strips made of different materials, amorphous carbon and fine grained polycrystalline aluminum. This double-strip substrate was placed onto the sample holder. In order to ensure a better thermal contact between holder and substrate we used indium spacers. The (115 ± 5) Å thick Al film served as an internal reference for the accurate determination of inter-plane distances. The carbon film was utilized to obtain accurate integrated intensities, avoiding the overlap of strong CO_2 lines with reflections from aluminum. The purity of the source co gas was better than 99.9%.

Before deposition the substrate was kept for 10 min at 45 K, whereupon then a sample was grown at that temperature. Then the temperature was raised to 55 K at a rate of 1 K/min and the sample was annealed for 5 min. After that the temperature was brought down to 5.6 K at a rate of 2 K/min and the sample was kept at that temperature for 10 min. The diffraction patterns were recorded at 45 K right after annealing and then during warm up at nine different temperatures from 6 to 70 K. The time needed for equilibration in every temperature point was at all times about 3 min. In order to reduce effects of the electron beam, we employed the highest accelerating voltage possible of 80 kV, thereby reducing the duration of the time an electron interacts with the sample. For the same purpose we used a Faraday cylinder, which shut the beam off during temperature stabilization processes and ensured extra control of the beam stability. The photo takings were analyzed on an IZA-2 optical comparator; the reflection intensities were determined after densitometric runs using an IFO-451 photometric device.

The sample temperature was varied with the aid of a dc heater at a fixed helium pumping rate. Temperature measurements were performed with a semiconductor thermometer, which was in good thermal contact with the substrate. The temperature measurement accuracy was not worse than ± 0.25 K over the temperature range 5 to 75 K. The CO_2 film thickness, which was typically about (450 ± 50) Å, was first controlled and subsequently evaluated from the following data: (i) the pressure of the gas in the filling container (close to 200 Torr as measured by an oil manometer); (ii) deposition time (about 30 s); (iii) the amount of the material deposited (an equivalent of about 1 Torr pressure drop); (iv) the orientation of the gas jet respective to substrate (usually, at an angle of $(45 \pm 5)^\circ$); (v) the distance between the filling pipe opening and the substrate (typically about 18 mm). Such a regime allowed us to grow polycrystalline CO_2 films with the characteristics that were close to those of «bulk» carbon dioxide crystals.

During experiments, when the helium vessel of the cryostat was filled to a sufficient level, the pressure in the column did not exceed $3 \cdot 10^{-7}$ Torr. To prevent the condensation of residue gases, the working chamber was protected by two screens, one at the liquid-nitrogen and the other, at liquid-helium temperature, which actually were additional cryopumps. During the whole diffraction experiment both intensity and focusing of the electron beam did not change.

4. Calculations

In this Section we describe some details of our method employed to reconstruct the absolute values of the orientational order parameters. This is necessary for the assessment of the validity of the method.

Table 1. Assessment of the accuracy of the approximating truncations for particular reflections observed in diffraction experiment. The lattice parameter a is that at $T = 0$.

Reflection j	Exact value [15] $F_{ex}^{(j)}$	$\Sigma_4^{(j)}$	$\Delta_4^{(j)}$ (%)	$\Sigma_6^{(j)}$	$\Delta_6^{(j)}$ (%)
111	4.3392708	4.3626179	0.5380426	4.3392043	– 0.0015334
200	2.5809769	2.6102143	1.1328012	2.5801121	– 0.0335058
210	– 3.084531	– 3.1331715	1.57692	– 3.0862019	0.0541703
211	–2.106178	– 2.0634765	– 2.0274837	– 2.1032798	–0.1376497
220	1.9100776	1.6408049	– 14.097477	1.9047396	– 0.2794693
311	0.3772583	0.431169	14.2901061	0.3907192	3.5680792
222	1.5078859	2.1396547	41.8976518	1.5049553	–-0.194354
320	– 2.2477249	– 2.4510779	9.0470569	– 2.2344827	– 0.5891404
321	– 1.5319902	– 1.4051779	– 8.2776198	– 1.5263462	– 0.3684124

4.1. Truncation accuracy evaluation

Exactly as done for diatomic cryocrystals [2,3,5], for the first step we do as follows. We set all the molecules rigidly oriented along the respective axes in the sublattices, which corresponds to the case $\eta = \eta_4 = \eta_6 = 1$ and all the off-diagonal orientational order parameters ζ_{ik} are zero. The relevant exact expressions as functions of the pertaining crystallographic and diffraction parameters for this case are well known [15]. The corresponding values, designated for particular reflections j as $F_{ex}^{(j)}$, are used for comparison with the respective approximations resulting from a particular truncation of the series in Eq. (5). These evaluations are summarized in Table 1. The notation is as follows. The scattering amplitude terms $F_s^{(n)}$ are defined in Eqs. (10) through (13);

$$\Sigma_N^{(j)} \equiv \sum_{n=0}^{N} F_s^{(n)} \tag{16}$$

and $\Delta_N^{(j)} \equiv \Sigma_N^{(j)} / F_{ex}^{(j)} - 1$ is the mismatch for a particular approximation of rank N for reflection j.

As one can see from Table, the approximation that accounts for the terms up to $N = 4$ is acceptable within a 2% error only for the four reflections with the least indices, *viz*., 111, 200, 210, and 211. To correctly calculate the scattering amplitudes for the other five reflections mentioned in Table, account of the term with $N = 6$ is necessary. Considering also a larger uncertainties in experimentally determined intensities for those five reflections, we did not use them in the subsequent reconstruction of absolute order parameter values.

4.2. Reconstruction of order parameters

Thus, the reconstruction procedure dealt with the four small-angle reflections. We sought two unknown values, the orientational order parameters η_2 and η_4, treating η_6 as known and equal to either 1 or, within a more precise approach, to a value found as explained in Appendix B. These two values were found as solutions to the following two equations, which are intensity ratios of reflections i and j represented by the truncated expansions of the scattering amplitudes with explicit unknowns η_2 and η_4. These theoretical ratios were equated to the values $R(i/j)$ known from experimental data:

$$\frac{I^{(i)}}{I^{(j)}} \simeq$$

$$\simeq \frac{f_i(T)\Phi_i P_i |F_0^{(i)} + \eta_2 F_2^{(i)} + \eta_4 F_4^{(i)} + \eta_6 F_6^{(i)}|^2}{f_j(T)\Phi_j P_j |F_0^{(j)} + \eta_2 F_2^{(j)} + \eta_4 F_4^{(j)} + \eta_6 F_6^{(j)}|^2} = R(i/j) \tag{17}$$

Here all quantities Φ, P, F_n, f were defined above in Eqs. (2), (10)–(13). Since η_6 is treated as known, a set of two equations like Eq. (17) involving at least three different reflections are needed to find η_2 and η_4.

5. Results and discussion

We have carried out six series of experiments, producing over 100 photo plates. In Fig. 1 we present a typical electron diffraction pattern. We used amorphous carbon for the substrate material and made it as thin as possible in order to reduce the incoherent scattering background, which is quite insignificant in the pattern depicted. Thus,

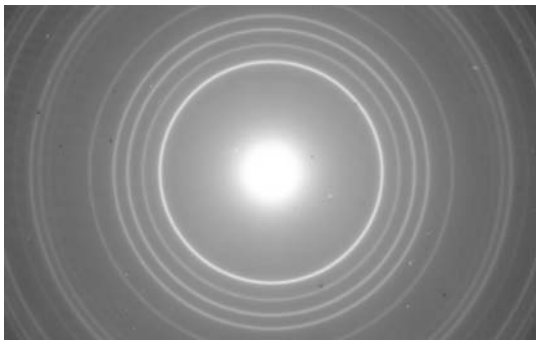

Fig. 1. THEED pattern from solid CO_2 on an amorphous carbon substrate; $T = 60$ K.

the inevitable small-angle halo is not seen. Here we also mark the absence of any appreciable effects of texture, multiple scattering. The rings are perfectly uniform and nicely circularly shaped, which is evidence of a high sample quality.

Diffraction patterns like that in Fig. 1 were next run through a standard densitometric procedure. The resulting patterns in electronic form were reduced to leave only fractions that contained the four reflections of interest, namely, 111, 200, 210, and 211. These shortened patterns were further processed to resolve them into individual reflections in order to evaluate their intensities. The fitting was performed using the Lorentzian line shape, which yielded a much better result compared to the Gaussian one, which also suggests a good sample quality. The final fitting is shown in Fig. 2. The experimental data run nicely along the fitting curve, the deviation not exceeding 1%. Ratios of these intensity values were further utilized to reconstruct the absolute values of the orientational order parameters η_2 and η_4. Since we dealt only with four reflections, by combining three of them in the respective set of two equations like Eq. (17), we could obtain six independent pairs of η_2 and η_4 values. The average of those four values was taken to be its true value, reconstructed from diffraction experiments.

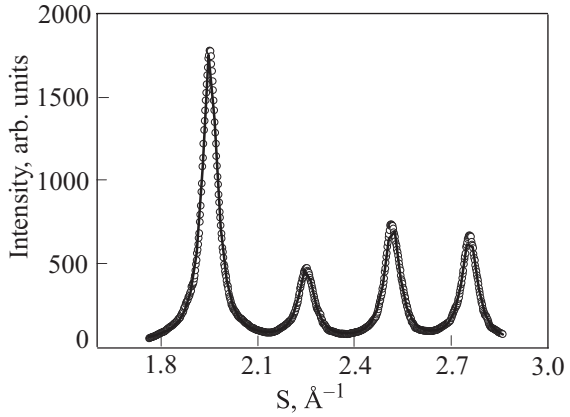

Fig. 2. An example of the intensity distributions from a solid CO_2 sample at $T = 60$ K.

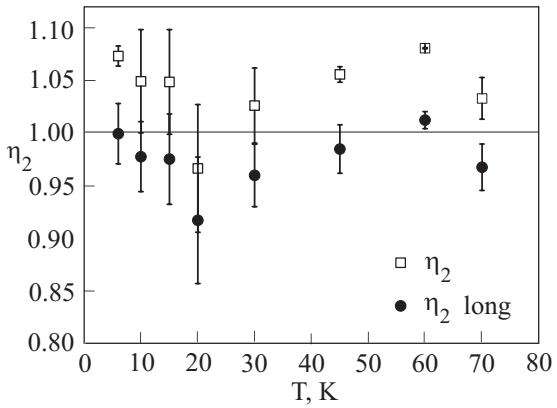

Fig. 3. Temperature dependence of the orientational order parameter η_2 of solid CO_2. The effective $2d$ values: 2.3198 Å (squares) and 2.4198 Å (circles).

The temperature dependence of the orientational order parameter η_2, as determined according to the procedure just described, is shown in Fig. 3 as empty squares. Almost all the values exceed unity, which is physically impossible. This fact suggests that we miss some factor that could bring the values to a physically reasonable level. One of such factors could be the fact that we use an isotropic Debye–Waller temperature factor $f_i(T)$, although in fact it might be anisotropic. However, variation of $f_i(T)$ did not lead to appreciable changes in the resulting η_2 values. There is another factor of importance. As mentioned above, for the half of the internuclear spacing in the molecule we employed the value $d = 1.1599$ Å derived from optical measurements [9]. We argue that instead we should use an effective value d_{eff} which is by a few percent larger than d. The argument leans on the speculation that electrons are scattered on the electron cloud, the size of which exceeds the internuclear spacing. If we put $d_{\text{eff}} = 1.04d$, we arrive at the η_2 values shown as solid circles in the same Fig. 3. Such a modification does not affect the general behavior of the $\eta_2(T)$ dependence, which is nonmonotone with a distinct dip at about $T = 20$ K. We are confident that this behavior reflects some changes that take place in the rotational and vibrational dynamics of the co crystal.

Figure 4 represents the temperature dependence of the rank-4 orientational order parameter η_4. As with η_2 in Fig. 3, the estimated values are too high; in order to bring them down we used the same renormalized value $d_{\text{eff}} \simeq 1.04\, d$ for the effective internuclear distance in the molecule. Again, the temperature dependence of η_4 exhibits a dip close to 20 K. Compared to η_2 as a function of temperature, the rank-4 order parameter shows a much steeper decrease, which is in accord with our reasonings in Appendix B. We should stress that the dip minimum at around 20 K and the maximum at 60 K in both η_2 and η_4 as a function of temperature were persistent for all series.

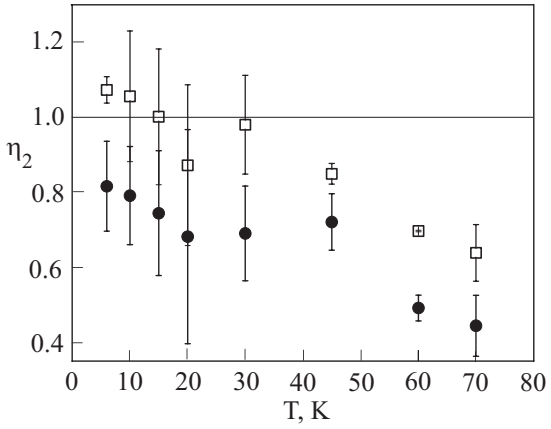

Fig. 4. Temperature dependence of the orientational order parameter η_4 of solid CO_2. The effective $2d$ values: 2.3198 Å (squares) and 2.4198 Å (circles).

It should be noted that the anomalies observed in this study correlate with the anomalies in the dilatometric expansivity data by Manzhelii et al. [13]. The heat capacity *versus T* curve also has an inflection, which might reflect a nonmonotone variation of η_2 with T. The rank-4 orientational order parameter η_4 is an important parameter, which determines the correlative and rotational-unharmonic effects in the librational subsystem, which are known to be large in triatomic molecular cryocrystals [16]. Detailed comparison of experimental η_4 values with theoretical estimates is needed.

We must also call attention to the temperature dependence of the cubic lattice parameter, which have been obtained in these measurements and depicted in Fig. 5. The values obtained by THEED are somewhat larger than those measured by powder x-ray diffraction, which is quite common, especially at low temperatures. But there is a kink at the lowest temperature, which is within the error bars shown but which was persistently observed for all runs.

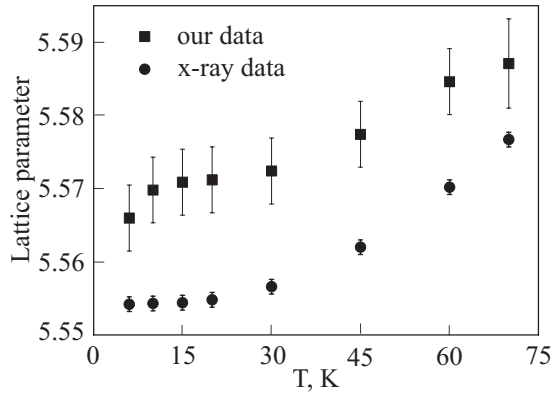

Fig. 5. Temperature dependence of the lattice parameter. The powder x-ray data are from Krupskii et al. [10].

6. Conclusions

The lattice parameter as well as the integrated reflection intensities of solid CO_2 have been determined by transmissive high-energy electron diffraction at temperatures from 6 to 70 K.

The method of reconstruction of absolute orientational order parameter values has been modified for the case of the triatomic CO_2 cryocrystal. It is shown that, because of the comparatively large length of the CO_2 molecule, a consistent description of the integrated intensity data can be obtained only if an orientational order parameter of a higher (fourth) rank, η_4 is taken into consideration together with the standard (rank-2) order parameter η_2.

Both orientational order parameters η_2 and η_4 in pure CO_2 have been reconstructed for temperatures from 6 to 70 K. A self-consistent reconstruction of these values was possible only if the internuclear distance in the CO_2 molecule, $2d$, is taken to be slightly (by about 4%) longer than determined spectroscopically. The order parameter η_4, determined for the first time in this work, is responsible for correlative effects in the thermodynamics and rotational dynamics of solid CO_2.

The authors are grateful to N.N. Galtsov for helping with data processing.

Appendix A: Transformations of spherical harmonics

To average $A_{2m} \equiv \langle C_{2m}(\mathbf{w}_c)\rangle$, it is convenient to rotate the reference frame so that its axis z would be directed along the 3-fold axis (one of the cube diagonals) of the $Pa\bar{3}$ structure, which is the natural frame for sublattice c. Then the value in the old frame is expressed via the value in the new, natural frame as

$$\langle C_{2m}(\mathbf{w}_c)\rangle = \sum_{m'} D^{2*}_{m,m'}(\chi)\langle C_{2m'}(\mathbf{w}_{c0})\rangle . \qquad (A.1)$$

Here χ is the set of Eulerian angles that effectuate the rotation; $D^{2*}_{m,m'}(\chi)$ is the Wigner functions [8]; $\mathbf{w}_{c0}$ is the unit vector along the molecular axis in the new reference frame. All components of $\langle C_{2m'}(\mathbf{w}_{c0})\rangle$ except that with $m = 0$ will average to zero from symmetry considerations, namely, because the maximum value of m, which is 2, is less than the order of the symmetry axis. The $m = 0$ average is exactly η as defined in Eq. (1). Now, since [8]

$$D^{2*}_{m,0}(\chi) = C_{2m}(\mathbf{m}_c), \qquad (A.2)$$

where $\mathbf{m}_c$ is the unit vector along the cube diagonal chosen in the «old» reference frame, which brings us to Eq. (8).

On the example of the term with $l = 4$ we show the emerging distinctions in the terms of higher orders. Now, in the expression $\langle C_{4m'}(\mathbf{w}_{c0})\rangle$ not only the $m' = 0$ term is nonzero. The presence of the 3-fold axis allows terms with $m = \pm 3$ to survive as well. Since the scalar

product $(\mathbf{C}_4(\mathbf{n})\cdot\mathbf{C}_4(\mathbf{w}_c))$ is invariant under rotation, we may consider this product in the intrinsic frame for the respective sublattice. Finally, this scalar can be recast to (we provide vectors in the intrinsic reference frame with subscript 0):

$$\sum_m C^*_{4m}(\mathbf{n})\langle C_{4m}(\mathbf{w}_c)\rangle =$$

$$= \sum_m C^*_{4m}(\mathbf{n}_0)\langle C_{4m}(\mathbf{w}_{c0})\rangle = \eta_4 P_4(\mathbf{n}\cdot\mathbf{m}_c) +$$

$$+ \frac{[\langle C_{43}(\mathbf{w}_{c0})\rangle - \langle C_{4\bar{3}}(\mathbf{w}_{c0})\rangle]}{2} \times [C^*_{43}(\mathbf{n}_0) - C^*_{4\bar{3}}(\mathbf{n}_0)] +$$

$$+ \frac{[\langle C_{43}(\mathbf{w}_{c0})\rangle + \langle C_{4\bar{3}}(\mathbf{w}_{c0})\rangle]}{2} \times [C^*_{43}(\mathbf{n}_0) + C^*_{4\bar{3}}(\mathbf{n}_0)]. \quad (A.3)$$

By suitably choosing the origin of the variable ϕ we are able to nullify the last term in Eq. (A.3) and bring it to the form

$$\sum_m C^*_{4m}(\mathbf{n})\langle C_{4m}(\mathbf{w}_c)\rangle =$$

$$= \eta_4 P_4(\mathbf{n}\cdot\mathbf{m}_c) + \zeta_{43}[C_{43}(\mathbf{n}_0) - C_{4\bar{3}}(\mathbf{n}_0)]. \quad (A.4)$$

Here η_4 is a rank-4 generalization of the orientational order parameter, Eq. (1), and we introduced a real-valued quantity with the proper subscripts,

$$\zeta_{43} \equiv \frac{\langle C_{43}(\mathbf{w}_{c0})\rangle - \langle C_{4\bar{3}}(\mathbf{w}_{c0})\rangle}{2}, \quad (A.5)$$

which characterizes the anisotropy of librations respective to the intrinsic frame.

Appendix B: Evaluation of order anisotropy parameters

Let us evaluate a typical anisotropy parameter, for example, ζ_{43}. The distribution function $\rho(x,\phi)$ of the orientational variables $x = \theta$ and ϕ, which in the intrinsic reference frame is centered around $\theta = 0$, can be expanded as

$$\rho(x,\phi) = \rho_0(x) + \sum_n \rho_n(x)\cos n(\phi - \phi_n), \quad (B.1)$$

where, by symmetry, any positive nonzero n is a multiple of 3. It is self-evident that the amplitudes $\rho_n(x)$ do not exceed in magnitude the main isotropic amplitude $\rho_0(x)$. In classical cryocrystals made up of linear molecules, in which the distribution is sharp around the value $x = 1$, $\rho_0(x)$ can be approximated as

$$\rho_0(x) \simeq \frac{1}{\kappa\pi^{3/2}} \exp\left[-\frac{(1-x)^2}{\kappa^2}\right], \quad (B.2)$$

where κ is the rms libration amplitude, which is small even in the ordered phases of nitrogen and carbon monoxide, not to mention co under discussion, i.e., the characteristic deviation $\Delta \equiv 1 - \eta$ is small compared to unity. If Δ is sufficiently small, then $\eta_4 \simeq 1 - (10/3)\delta$. Here we make a general remark that the higher order parameters are more sensitive to deterioration of the orientational order. The quantity Δ is easily related with κ: $\Delta = 3\kappa\pi^{-1/2}$. Averaging of $C_{43}(\mathbf{w}) = P_{43}(x)e^{3i\phi}$, where $P_{43}(x)$ is the respective associated Legendre polynomial, gives $\langle C_{43}(x)\rangle \simeq 1.46\Delta^2$. In N_2 close to the orientational transition point [14], $\Delta \simeq 0.27$ so that $\langle C_{43}(x)\rangle \simeq 0.106$ is substantially smaller than $\eta = 0.73$ or smaller even than $\eta_4 \simeq 0.39$. There are solid grounds to expect that in co $\langle C_{43}(x)\rangle$ will be more negligible compared to the rank-4 isotropic order parameter η_4.

1. M.A. Strzhemechny, A.A. Solodovnik, and S.I. Kovalenko, *Fiz. Nizk. Temp*. **24**, 889 (1998) [*Low Temp. Phys*. **24**, 669 (1998)].
2. N.N. Galtsov, O.A. Klenova, and M.A. Strzhemechny, *Fiz. Nizk. Temp*. **28**, 517 (2002) [*Low Temp. Phys*. **28**, 365 (2002)].
3. V.V. Danchuk, N.N. Galtsov, M.A. Strzhemechny, and A.I. Prokhvatilov, *Fiz. Nizk. Temp*. **30**, 163 (2004) [*Low Temp. Phys*. **30**, 118 (2004)].
4. J.L. Yarnell, R.L. Mills, and A.F. Schuch, *Fiz. Nizk. Temp*. **1**, 760 (1975) [*Sov. J. Low Temp. Phys*. **1**, 366 (1975)].
5. A.A. Solodovnik, V.V. Danchuk, and M.A. Strzhemechny, *J. Non-Cryst. Solids* **352**, 4331 (2006).
6. M.A. Krivoglaz, *Theory of Scattering of x-rays and Thermal Neutrons by Real Crystals*, Nauka, Moscow (1967) [in Russian].
7. G.B. Bokii and M.A. Porai-Koshitz, *X-ray Structure Analysis*, Moscow University (1964) [in Russian].
8. L.V. Gurvich et al., *Thermodynamic Properties of Individual Substances*, Vol. 2, Book 1, Nauka, Moscow (1979).
9. I.N. Krupskii, A.I. Prokhvatilov, A.I. Erenburg, and A.S. Barylnik, *Fiz. Nizk. Temp*. **8**, 533 (1982) [*Sov. J. Low Temp. Phys*. **8**, 263 (1982)].
10. D.A. Varshalovitch, A.N. Moskalev, and V.K. Khersonskii, *Theory of Angular Momentu*m, World Scientific, Singapore (1988).
11. M.A. Strzhemechny, *J. Low Temp. Phys*. **139**, 581 (2005).
12. B.K. Vainshtein, *Structural Analysis by Electron Diffraction*, Pergamon, Oxford (1964).
13. V.G. Manzhelii, A.M. Tolkachev, M.I. Bagatskii, and E.I. Voitovich, *Phys. Status Solidi* **B44**, 39 (1971).
14. T.A. Scott, *Phys. Rep*. **C27**, 89 (1976).
15. *International Tables for x-ray Crystallography, vol. 1, Symmetry Groups*, N.F.M. Henry and K. Lonsdale (eds.), Kynoch Press, Birmingham (1969).
16. *The Physics of Cryocrystals*, V.G. Manzhelii, Yu.A. Freiman, M.L. Klein, and A.A. Maradudin (eds.), AIP Press, Woodbury (1997).